Available online at www.sciencedirect.com
ScienceDirect
European Journal of Medicinal Chemistry 44 (2009) 834–844
EUROPEAN JOURNAL OF MEDICINAL CHEMISTRY
http://www.elsevier.com/locate/ejmech

Original article

Synthesis and characterization of dinuclear macrocyclic cobalt(II), copper(II) and zinc(II) complexes derived from 2,2,2′,2′-*S*,*S*[bis(bis-*N*, *N*-2-thiobenzimidazolyloxalato-1,2-ethane)]: DNA binding and cleavage studies

Farukh Arjmand*, Mubashira Aziz

Department of Chemistry, Aligarh Muslim University, Aligarh 202002, Uttar Pradesh, India

Received 25 April 2008; accepted 5 May 2008
Available online 16 May 2008

Abstract

New homodinuclear macrocyclic complexes of cobalt(II), copper(II) and zinc(II) were isolated from the newly synthesized ligand 2,2,2′,2′-*S*,*S*[bis(bis-*N*,*N*-2-thiobenzimidazolyloxalato-1,2-ethane)]. The structures of the complexes were elucidated by elemental analysis, molar conductance measurements, IR, ^{1}H NMR, ^{13}C NMR, electronic and ESI-MS spectroscopic techniques. In complex **1**, Co(II) ions possess a tetrahedral coordination environment composed of O_2S_2 donor atoms while its Cu(II) and Zn(II) counterparts **2** and **3**, respectively, reveal a six coordinate octahedral structure, defined by the O_2S_2 donors from the macrocyclic ring and two chloride ions. Molar conductance and spectroscopic data also support the proposed geometry of the complexes. DNA binding properties of complexes **1**–**3** were investigated using electronic absorption spectroscopy, fluorescence spectroscopy, viscosity measurements and cyclic voltammetry. The absorption spectra of complexes **2** and **3** with calf thymus DNA showed hypochromism, while complex **1** showed hyperchromism attributed to a partial intercalation and electrostatic binding modes, respectively. The intrinsic binding constant K_b of complexes **1**–**3** were determined as $16.6 \times 10^4\ M^{-1}$, $4.25 \times 10^4\ M^{-1}$ and $3.0 \times 10^4\ M^{-1}$, respectively. The decrease in the relative specific viscosity of calf thymus DNA with increasing concentration of the complexes authenticates the partial intercalation binding mode. Gel electrophoresis of complex **2** with plasmid DNA demonstrated that complex exhibits excellent ''artificial'' nuclease activity.

Keywords: Benzimidazole macrocylic complexes; UV–vis; Flourescence; Artificial cleavage activity; CT-DNA; Plasmid DNA; Drug candidates

1. Introduction

Medicinal inorganic chemistry is an area of growing interest owing to the fact that inorganic pharmaceuticals play a key role in clinical therapy (e.g. cisplatin and second generation alternatives carboplatin and oxaliplatin – chemotherapeutic agents for solid malignancies) and diagnostics (e.g. MRI contrast agents) [1]. For these inorganic compounds, the metal serves as structural center for organizing the organic ligands in the biologically relevant chemical space [2]. Transition metals appear more appealing for this purpose because they can support a multitude of coordination numbers and geometries that go far beyond sp, sp^2 and sp^3 hybridizations of carbon [3]. Another key aspect for using metal containing compounds as structural scaffolds is the kinetic stability of the coordination sphere in the biological environment [4]. Among the ligands employed for drug design, benzimidazole nucleus serves as an important pharmacophore in drug discovery [5]. Benzimidazoles are very useful subunits for the development of molecules of pharmaceutical or biological interest. Substituted benzimidazole derivatives have diverse therapeutic applications as they exhibit antihistamine, antiulcerative,

Abbreviations: bzim, Benzimidazole; CT-DNA, calf thymus DNA; CV, cyclic voltammetry; EB, ethidium bromide; LNT, liquid nitrogen temperature; TCNE, tetracyanoethylene.

* Corresponding author.
E-mail address: farukh_arjmand@yahoo.co.in (F. Arjmand).

0223-5234/$ - see front matter © 2008 Elsevier Masson SAS. All rights reserved.
doi:10.1016/j.ejmech.2008.05.006

antifungal, antioxidant, antiinflammatory, antitumor, antikinase and potential anticancer activities [6]. The biological relevance of these heterocyclic aromatic building blocks is due to their structural similarity to purine nucleobase and also as benzimidazole derivatives selectively inhibit endothelial cell growth and suppress angiogenesis in vitro and in vivo [7].

Bis(imidazol-2-yl)methane (BIM), in which two imidazole rings are linked via the methylene group is reported to be very effective complexing agents for various transition metal ions, forming stable six membered chelates via nitrogen donor atoms [8]. Similarly, tetradentate ligands viz, bis(pyrid-2-yl)-/bis(benzimidazol-2-yl)-dithioethers provide donor atoms such as imidazole nitrogen and thioether sulphur to fine tune the electronic and DNA binding properties of metal complexes [9]. Since DNA has been identified as the primary molecular target [10] of metal based anticancer drugs, interaction of well tailored metal complexes with DNA ascertains the extent and mode of DNA binding and the potential of these complexes to act as chemotherapeutic agents. There are various modes of DNA interaction – covalent, non-covalent, intercalation etc. DNA targeted metal based drugs which involve covalent binding to nucleobase moieties have shown low degree of selectivity [11]. Recently, non-covalent DNA binding metal complexes particularly metallointercalators have received attention in the development of efficient anticancer drugs [12]. Intercalation is well known to strongly influence the properties of the DNA and has been reported as a preliminary step in mutagenesis [13]. In this work, we aim to study the DNA binding properties of new cobalt, copper and zinc macrocycles derived from benzimidazole ligands. Copper, cobalt and zinc are essential metal ions and play crucial roles in biological and biomedical processes. Copper complexes which possess biologically accessible redox potentials, demonstrate high nucleobase affinity and are reported to be novel oxidative cleaving agents of DNA [14,15]. The binding of complexes **1–3** with calf thymus DNA has been investigated by spectroscopic methods, cyclic voltammetry and viscosity measurements. Interaction of complex **2** with plasmid circular DNA (pBR322 DNA) employing gel electrophoresis demonstrated its ''artificial'' nuclease activity or nuclease like activity.

2. Results and discussion

2.1. Chemistry

Ligand L_2 and its metal complexes **1–3** were synthesized by a procedure as illustrated in Scheme 1. Formulations of the ligand and the complexes were verified by elemental analysis, molar conductivity as well as by UV–vis, mass and NMR spectroscopies. Molar conductance measurement of the complexes in DMSO corresponds to the 1:4 electrolytic natures for complex **1** while complexes **2** and **3** behave as non-electrolytes. Evidently, in complexes **2** and **3** the metal ions are hexacoordinated surrounded by $O_2S_2Cl_2$ environment, adopting an octahedral geometry, while in complex **1** the Co(II) ions are in tetrahedral environment with O_2S_2 donor set, confirmed by UV–vis and mass spectral data. Complexes **1–3** and ligands L_1 and L_2 were soluble in DMF, DMSO and MeOH, respectively. Energy minimized structure using CS Chem Draw 3D Pro 5.0 as shown in Fig. 1 validated the

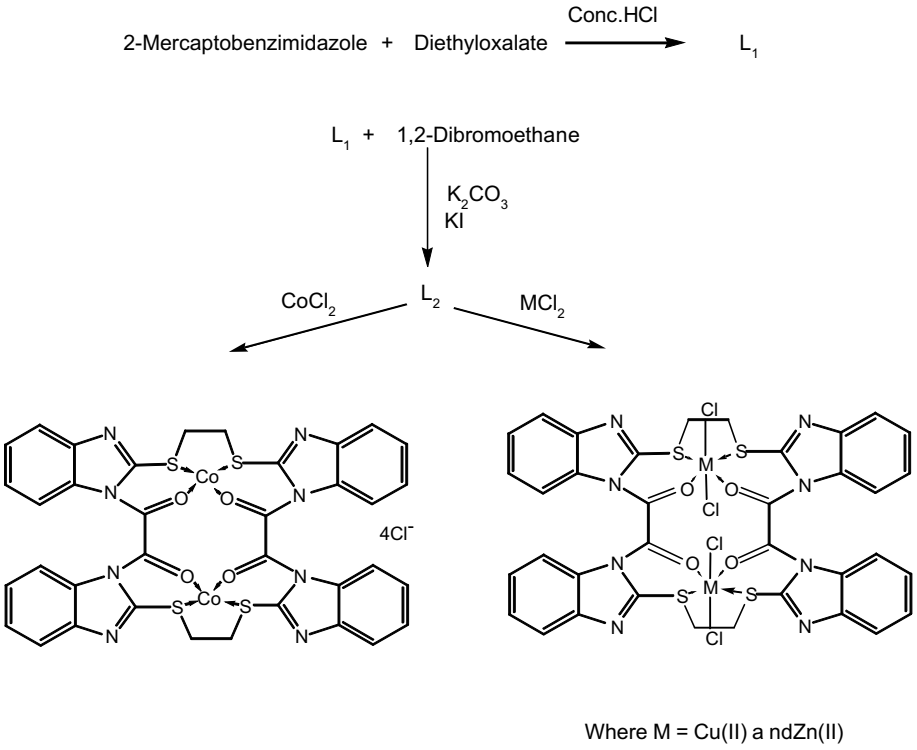

Scheme 1.

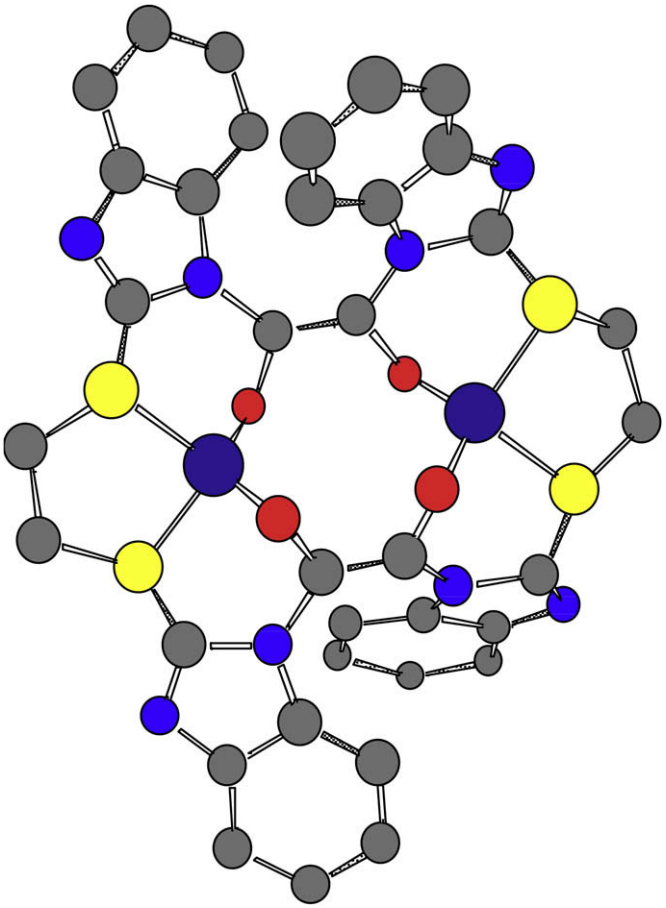

Fig. 1. Molecular model of complex **1**.

proposed structures. DNA binding studies were performed with Co(II) (**1**), Cu(II) (**2**) and Zn(II) (**3**) complexes.

2.1.1. Infrared spectra

The IR spectrum of ligand L_1 exhibited a characteristic band at 2368 cm^{-1} attributed to the ν(S–H) vibrations [16], indicating that the thiol proton remains attached to the sulphur atom. However, the absence of ν(N–H) stretching band at ~3400 cm^{-1} [17] implies its deprotonation and subsequent ligand formation with diethyloxalate. The presence of an intense ν(C=O) stretching absorption detected at 1625 cm^{-1} confirms the bridging of the two imidazole rings [18]. Two medium intensity bands at 1523 cm^{-1} and 1353 cm^{-1} were assigned to the ν(C=N) and ν(C–N), respectively [19]. The IR spectrum of ligand L_2 was quite similar to L_1 except for the missing peak at 2368 cm^{-1} due to the –SH group. The deprotonation of thiol groups was also inferred from the presence of a broad band at ca. 2853 cm^{-1} belonging to the νCH_2 of the aliphatic chain. Additionally, the pure characteristic ν(C–H) modes of the ring residues in L_1 and L_2 were observed in the wave regions at 3100 cm^{-1}. The IR spectra of complexes **1**–**3** reveal slight but specific differences from the spectra of free ligands. On complexation, the shifting of the ligand ν(C=O) and ν(C–S) bands towards the lower side suggests the involvement of oxygen and sulphur atoms in coordination. Of particular interest is the lower frequency region, characteristic for the metal–chloride and metal–oxygen stretching vibrations. Complexes **1**–**3** display metal–oxygen bands at 493–509 cm^{-1}. The appearance of a band at ~455 cm^{-1} region in complexes **2** and **3** supports the formation of metal–chloride bonds while its absence in the IR spectrum of **1** indicates that the chloride ions do not participate in coordination and behave as counterions. This was also supported by the ESI-MS and conductivity measurements.

2.1.2. Nuclear magnetic resonance spectra

The formation of new macrocyclic complexes were also ascertained by ^1H and ^{13}C NMR spectra of ligands L_1, L_2 and complex **3**. The signal due to the –SH functionality appearing at 2.95 ppm in the free ligand spectrum of L_l was missing both in ligand L_2 and complex **3** [20]. The absence of the characteristic –NH proton signal of the imidazole ring at 12.00–14.00 ppm corresponds to the deprotonation of the –NH group. The observation of a singlet for methylene protons at 2.75 ppm [21] and a multiplet for the benzimidazole protons in the range 7.15–7.69 ppm indicated the equivalence of the two halves of ligand L_2. Compared with the free ligand, complex **3** showed proton signals at nearly identical positions. The ^{13}C NMR spectra of ligands L_1 and L_2 exhibited the carbonyl –C=O and ring carbon atoms of the imidazole moiety at 151.24–160.96 ppm and at 112.96–139.25 ppm, respectively. Signals at 39.5 ppm were ascribed to the S–CH_2–CH_2–S [22] carbons of ligand L_2. Complex **3** displayed spectral pattern similar to that of the ligands except downfield chemical shifts of carbon signals. The carbonyl signal was desheilded in the spectra of the metal complex which appeared at 164.27 ppm in comparison to 151.24 ppm in L_2, inferring coordination through the oxygen atom of the ligand. Significant chemical shift was also observed for –S–CH_2– resonances, which implies coordination via sulphur atoms. These observed spectral features conformed to the proposed macrocyclic structure.

2.1.3. Mass spectral analysis

The ESI-MS spectra of ligands L_1, L_2 and complex **1** were obtained in the acetonitrile solutions. The spectrum of ligand L_1 shows peaks at *m/z* 429 and 494 that were assigned to the ($C_{16}H_{10}N_4O_2S_2 \cdot 2HCl + 2H^+$) and ($C_{16}H_{10}N_4O_2S_2 \cdot 3HCl \cdot CH_3OH + H^+$) compounds, respectively. For ligand L_2, peaks centered at *m/z* 817 and 775 corresponded to $C_{36}H_{24}N_8O_4S_4 \cdot CH_3CN \cdot H_2O - 2H^+$ and $C_{36}H_{24}N_8O_4S_4 \cdot H_2O - 3H^+$ species, respectively. The ESI-MS spectrum of complex **1** shows molecular ion peak at *m/z* 1019. Peaks at *m/z* 981, 478, 222 and 224 correspond to the ion peaks resulting from the successive expulsion of the chloride ions from the complex entity. This implies that the chloride ions were not coordinated to the cobalt ion.

2.1.4. Electron paramagnetic resonance spectroscopy

The solid state X-band EPR spectrum of complex **2** acquired at LNT under the magnetic field strength 3000 ± 1000 guass with tetracyanoethylene (TCNE) as field marker ($g = 2.0027$) showed an anisotropic spectrum,

exhibiting both parallel and perpendicular g values. The EPR spectrum of complex **2** consists of a very broad axial symmetrical line shape with $g_{\|} = 2.16$, $g_{\perp} = 2.08$ values and $g_{av} = 2.106$ computed from the formula $g_{av}^2 = g_{\|}^2 + 2g_{\perp}^2/3$, suggesting an octahedral geometry [23]. The trend $g_{\|} > g_{\perp} > g_e$ (2.0023) revealed that the unpaired electron was located in the $d_{x^2-y^2}$ orbital of the Cu^{II} ions characteristic of axial symmetry. The parameter $G = (g_{\|} - 2)/(g_{\perp} - 2)$, measures the exchange interaction between the metal center in a polycrystalline solid. According to Hathaway and Billing [24] $G > 4$ indicate negligible exchange interaction in the solid complex. For the Cu(II) complex $G < 4$ indicates considerable exchange interaction in the complex.

2.1.5. Electronic absorption spectra

The electronic spectra of ligands L_1 and L_2 and their complexes were recorded in DMSO at room temperature. The UV region of the electronic spectra of the ligands, both free and in the coordinated form was dominated by a pair of bands, one intense and a narrow band at 270–290 nm and a second less intense band around 242–247 nm. The low energy UV band has been assigned to an intraligand $\pi \rightarrow \pi^*$ transition of the benzimidazolyl groups and the high energy UV band was ascribed to intraligand charge transfer transitions. In the visible region, complex **1** displays two bands, one low at 617 nm and a high at 680 nm assigned to $^4A_2 \rightarrow {}^4T_1$ transition, typical for tetrahedral Co(II) complexes [25]. The high value of the molar extinction coefficient and the blue colour of the Co(II) complex, also authenticate tetrahedral stereochemistry. On the other hand complex **2** showed a band with low extinction coefficient at 800 nm due to $^2B_{1g} \rightarrow {}^2A_{1g}$ transition [26] supporting an octahedral geometry around Cu(II) metal ion.

2.2. DNA binding studies

2.2.1. Absorption spectral studies

The binding of the metal complexes to DNA helix is often characterized through absorption spectral titration, followed by the changes in the absorbance and shift in the wavelength. The absorption spectra of **1**–**3** in the absence and presence of CT-DNA are illustrated in Fig. 2a–c, respectively. Upon the addition of CT-DNA to **1**–**3**, interesting changes in the absorbances of the intraligand absorption bands of the complexes were observed – hyperchromism for **1** and hypochromism for **2** and **3**. Hyperchromism and hypochromism are the spectral changes typical of a metal complex's association with the DNA helix [27,28]. The hypochromicity, characteristic of intercalation [29] has been usually attributed to the interaction between the electronic states of the compound chromophores and those of the DNA bases [30], while the red shift has been associated with the decrease in the energy gap between the highest and the lowest molecular orbitals (HUMO and LUMO) after binding of the complex to DNA [31]. The observed hyperchromism for **2** and **3** unambiguously revealed the active participation of bzim moieties in association with the DNA [32]. However, the lack of red shift suggests that the binding mode of both **2** and **3** was not classical intercalation. Because of the bulky structure of the complexes, the bzim rings cannot completely intercalate. When one of the four bzim rings inserts into the helix, the other rings extend away from the plane due to the stereochemistry effect and hence decreasing the effective area of overlap. Interestingly, complex **1**, inspite of containing bzim rings exhibits a hyperchromism, suggestive of electrostatic binding. Due to electrostatic binding on the DNA surface, it appears to undergo distortion in the coordination sphere resulting in the enhanced absorption intensity of the intraligand bands. Similar reports were observed for DNA binding studies of ruthenium complexes derived from tetradentate bis(benzimidazol-2-yl)dithioether ligands [33]. Therefore, the observed spectral changes were rationalized in terms of partial intercalation and electrostatic binding. To further illustrate the DNA binding strength, the intrinsic binding constant K_b was determined by Eq. (7) for complexes **1**–**3** which were found to be $16.6 \times 10^4\ M^{-1}$, $4.25 \times 10^4\ M^{-1}$ and $3.0 \times 10^4\ M^{-1}$, respectively. The binding constants of these complexes were lower in comparison to those observed for typical classical intercalators (ethidium-DNA, $1.4 \times 10^6\ M^{-1}$) [34]. The diminution of the intrinsic binding constants could be explained by the steric constraints imposed by the ligand framework and thus encouraging a partial intercalation binding mode for the complexes.

2.2.2. Fluorescence studies

Upon excitation at $\pi \rightarrow \pi^*$ transitions either in DMSO or in the presence of CT-DNA, complexes **1**–**3** cannot emit luminescence. Hence, steady state competitive binding studies of the three complexes were monitored by a fluorescent EB displacement assay. EB, a planar aromatic heterocyclic dye intercalates non-specifically into the DNA which causes it to fluoresce strongly [35].

$$\mathrm{EB(weakfluorescent)} + \mathrm{DNA(non-fluorescent)} \rightleftharpoons \mathrm{EB{-}DNA(strongfluorescent)}$$

Competitive binding of second DNA binding macromolecule results in the displacement of bound EB and a decrease in the fluorescence intensity, furnishing indirect evidence for the DNA binding mode. The emission spectra of EB bound DNA in the absence and presence of increasing amounts of complexes **1**–**3** are given in Fig. 3. The emission intensity of DNA–EB system ($\lambda_{em} = 590$ nm) decreases appreciably, which indicated that the compounds could replace EB from the DNA–EB system. Such a characteristic change is often observed in intercalative binding modes [36]. The quenching plots (inset) followed the Stern–Volmer relationship [37] of the form:

$$I_0/I = 1 + Kr \quad (1)$$

where I_0 and I are the fluorescence intensities of the excited DNA–EB in the absence and presence of the complexes, K is the Stern–Volmer quenching constant and r is the ratio of the concentration of the metal complexes to DNA. In the plot of I_0/I vs. [complex]/[DNA], K is given by the ratio of the slope to intercept. The K values for complexes **1**–**3** were found to be 0.04, 0.26 and 0.06, respectively.

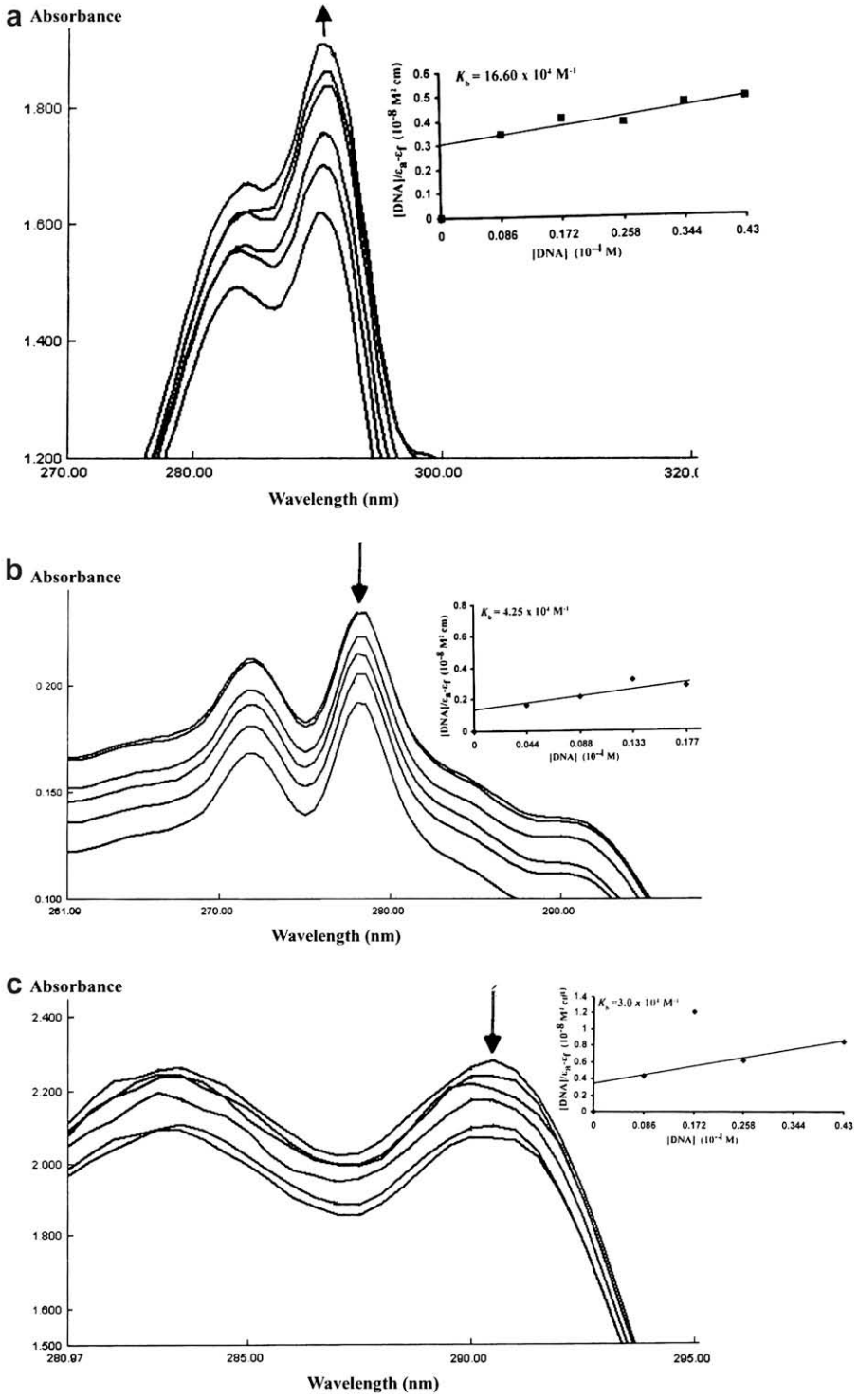

Fig. 2. Absorption spectral traces of (a) complex **1**, (b) complex **2** and (c) complex **3** in Tris–HCl buffer upon addition of CT-DNA. Inset: plots of $[DNA]/\varepsilon_a - \varepsilon_f$ vs. [DNA] for the titration of CT-DNA with complexes (◆), experimental data points; full line, linear fit of the data. [Complex **1**] and [complex **3**] = 0.33×10^{-4} M, [DNA] = $0.86–4.30 \times 10^{-5}$ M; [complex **2**] = 0.66×10^{-5} M, [DNA] = $0.44–2.21 \times 10^{-5}$ M.

The effect of complexes **1–3** on the fluorescence intensity of EB was also investigated in the presence of increasing amounts of DNA. The fluorescence intensity of EB has a gradual enhancement with the addition of DNA in the absence and presence of metal complexes. Fluorescence Scatchard plots [38] for the binding of EB to DNA in the presence of metal complexes (Fig. 4) were obtained from equation:

$$r_{EB}/C_{EB,f} = (n - r_{EB})[K_{EB}/1 + K_M] \quad (2)$$

where r_{EB} is the ratio of bound EB to total nucleotide concentration; $C_{EB,f}$, concentration of free EB; n, maximum value of r_{EB}, K_{EB} and K_M, intrinsic binding constants for EB and metal complexes to DNA, respectively, and $C_{M,f}$, concentration of

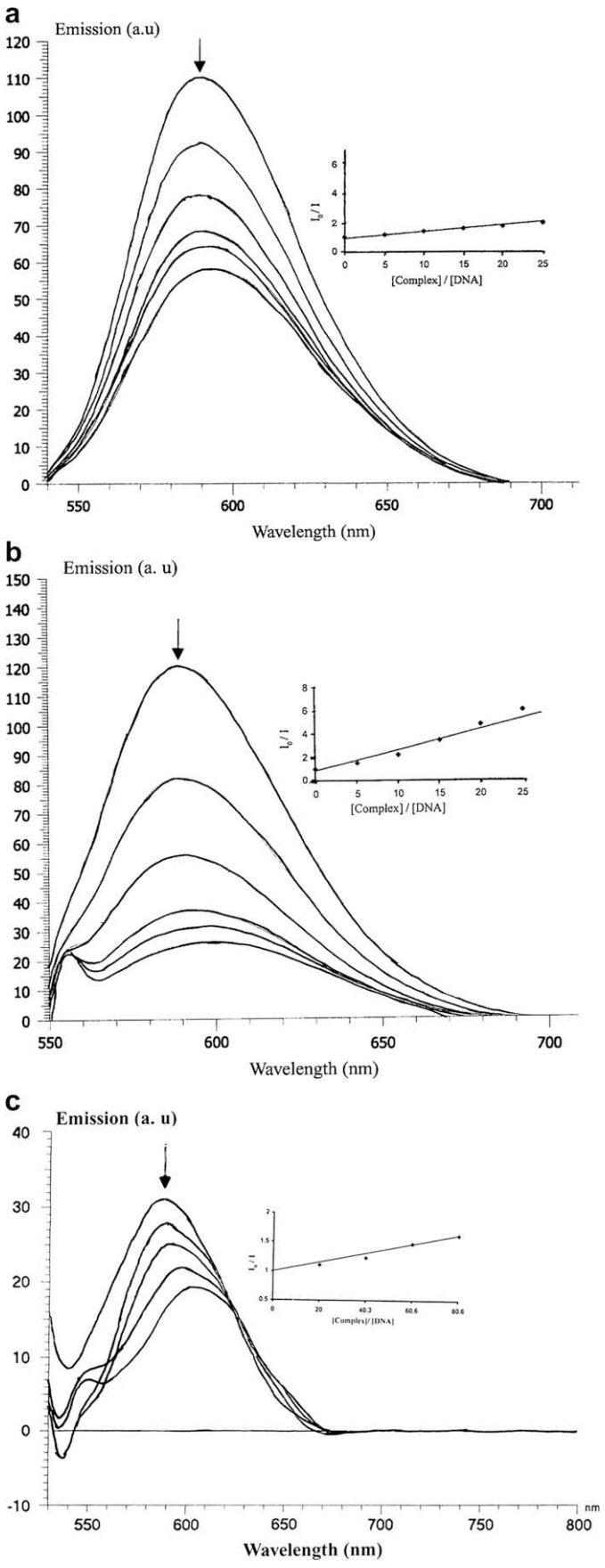

Fig. 3. Emission spectra of EB bound to DNA in the presence of (a) complex **1**, (b) complex **2** and (c) complex **3** in Tris–HCl buffer. Arrows indicate the intensity changes upon increasing concentration of the complexes. Inset: fluorescence quenching curve of DNA-bound EB with complexes (◆), experimental data points; full lines, linear fit of the data. [Complex **1**] and [complex **2**] = 0.33–1.66 × 10^{-4} M, [DNA] = 0.66 × 10^{-5} M, [complex **3**] = 0.66–2.66 × 10^{-4} M, [DNA] = 0.33 × 10^{-5} M; λ_{ex} = 510 nm.

free metal complex. Using fluorescence to obtain r_{EB}, binding isotherms were constructed. With the addition of the complexes, the slope that is K_{obs} decreases with the increase in the concentration of the complex indicating inhibition of EB binding.

From the above Eq. (2) we obtain the relationship:

$$K_{obs} = [K_{EB}/1 + K_M] \quad (3)$$

The reciprocal of Eq. (3) produces a straight line equation:

$$1/K_{obs} = (K_M/K_{EB})C_{M,f} + 1/K_{EB} \quad (4)$$

The concentration of free complexes were approximated from the following equation:

$$r_M = n - r_{EB} - r_{EB}/K_{EB}C_{EB} \quad (5)$$

$$C_{M,f} = C_M - r_M C_{DNA} \quad (6)$$

where r_M is the ratio of bound complex to total DNA concentration, $C_{M,f}$ and C_M are concentrations of free and total metal complexes, respectively. Replots of K_{obs} gave the approximate binding constants of complexes **1**–**3** which were calculated to be 2.49 × 10^3, 1.04 × 10^4 and 1.85 × 10^4, respectively (Fig. 5).

2.2.3. DNA cleavage activity

The chemical nuclease like activity of the copper(II) complex, **2** has been investigated by agarose gel electrophoresis using supercoiled pBR322 plasmid DNA as a substrate. The pBR322 DNA was mixed with different concentrations of **2** in Tris–HCl buffer in the absence and presence of reductant ascorbic acid and mixtures were incubated at 37 °C for 1 h. Control experiments using only complex or ascorbic acid failed to show any apparent cleavage activity. In the absence of ascorbic acid, pBR322 plasmid DNA was converted from SC (form I) to NC (form II), (Fig. 6a) revealing the efficient cleavage like activity and at higher concentrations of complex **2**, increased band intensities were observed. Since Cu(II) complexes are catalytically active in the oxidation of ascorbic acid by dioxygen involving Cu(I) intermediate species, we have examined the cleavage like activity of **2** in the presence of ascorbic acid at increasing concentration of the complex. There was complete conversion of SC form I to nicked DNA form (II) with almost disappearance of form (III). The bands are more intensified in the presence of ascorbic acid than in the absence of ascorbic acid as seen from Fig. 6b. The intense nuclease activity was apparently caused by enhanced stabilization of Cu(I) species formed upon its reduction by ascorbic acid. This supports oxidative cleavage mechanism of **2** where Cu(II) complex is first reduced by ascorbic acid to form the Cu(I) species, which then binds to DNA forming

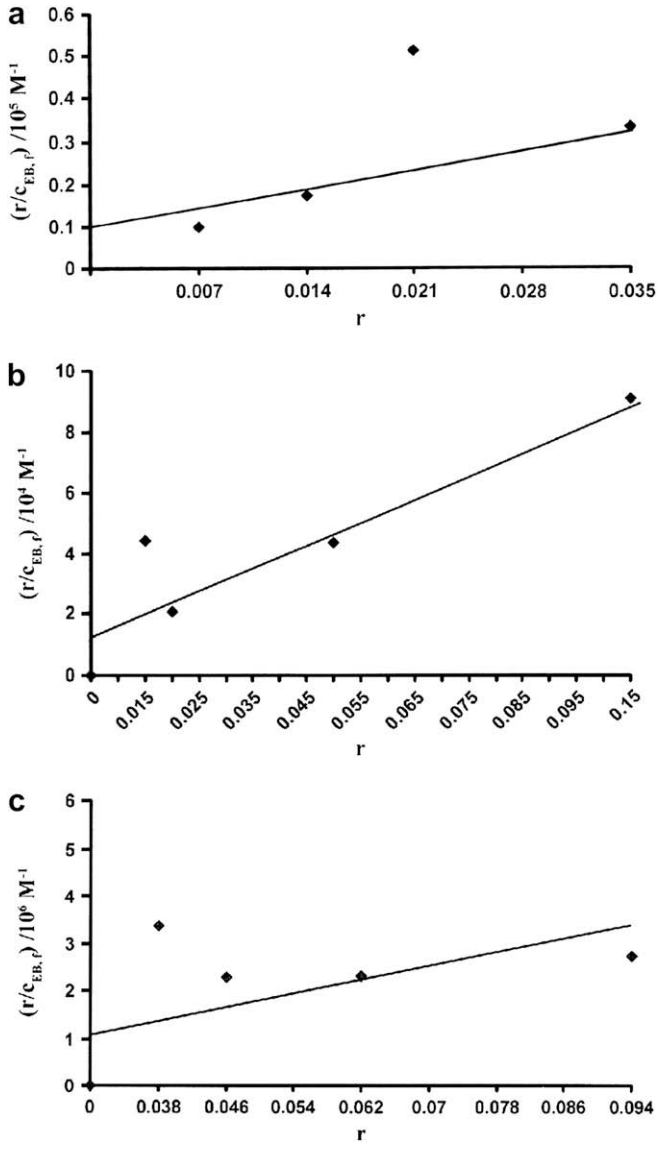

Fig. 4. Scatchard plots for the binding of EB to DNA in the presence of (a) 0.33×10^{-4} M, (b) 1.33×10^{-4} M, (c) 3.30×10^{-4} M of the representative complex **1**; [EB] = 0.66×10^{-6} M.

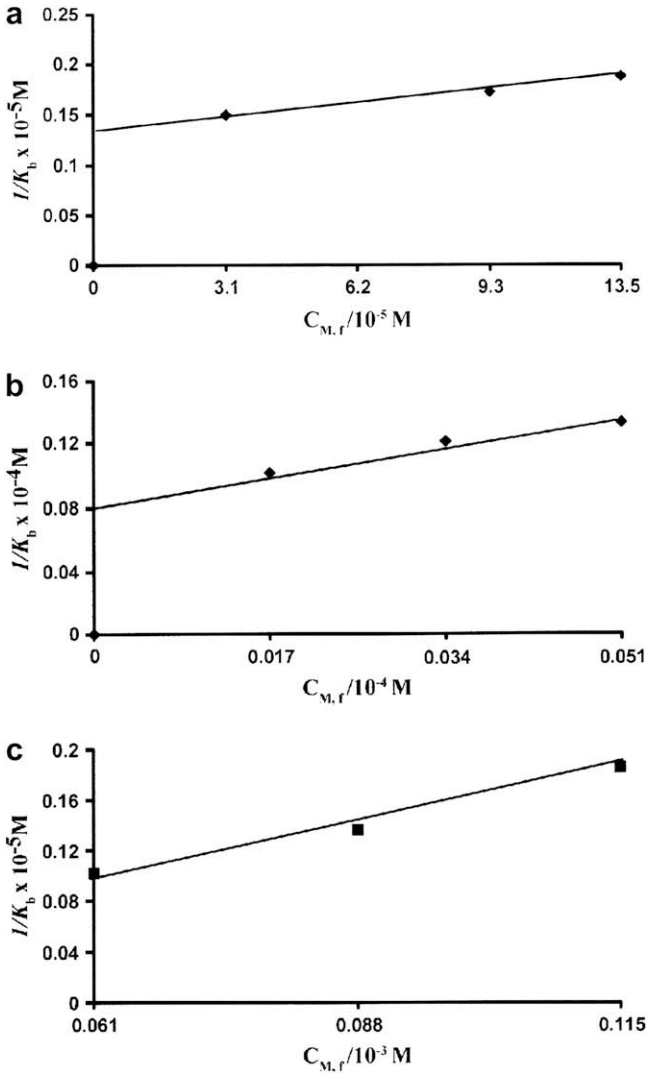

Fig. 5. Replot of observed binding constant of EB to DNA for (a) complex **1**, (b) complex **2** and (c) complex **3**.

a Cu(I)complex–DNA adduct. This adduct then reacts with dioxygen to form a peroxodicopper(II) derivative which could generate active oxygen species required for cleavage [39,40].

2.2.4. Viscosity studies

To further explore the interaction properties between the metal complexes and the DNA, the relative specific viscosity of DNA was examined by varying the concentration of the added metal complexes. Measuring the viscosity of DNA is a classical technique used to analyze the DNA binding mode in solution [41]. Hydrodynamic measurements i.e. viscosity, sedimentation, rotational diffusion, etc. sensitive to molecular lengths provide strong evidences for the DNA binding modes, especially in the absence of crystallographic and NMR structural data [42]. A classical intercalation model results in the lengthening of the DNA helix as the base pairs are separated to accommodate the binding molecule, leading to an increase in the DNA viscosity. In contrast, partial intercalators as well as covalent binders could bend or kink DNA helix, reduce its effective length and in turn its viscosity [43,44]. Fig. 7 depicts the effect of complexes **1–3** on the DNA viscosity. The plot reveals that the relative solution viscosity decreased with increasing concentration of the complexes, indicating that the DNA becomes more compact, resulting in DNA aggregation. The aggregation reduces the number of independently moving DNA molecules in solution and hence leads to a decrease in viscosity [45]. These results support that complexes **1–3** binds to CT-DNA by partial intercalation [46]. Further, due to the bulky structure of the complexes, they would act as a wedge to pry apart one side of a base pair stack but not fully separate the stack as required by the classical intercalation model.

2.2.5. Cyclic voltammetry

CV is an electroanalytical technique used to study the mechanistic behaviour of redox systems of new metal

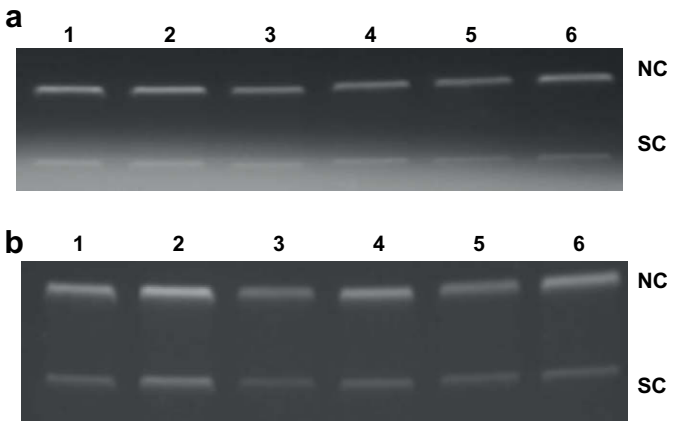

Fig. 6. Gel electrophoresis diagram showing cleavage of pBR322 supercoiled DNA (300 ng) by complex **2**: (a) in the absence of ascorbic acid; 250 μM **2** + DNA, (lane 1), 200 μM **2** + DNA (lane 2), 150 μM **2** + DNA (lane 3), 100 μM **2** + DNA (lane 4) and 50 μM **2** + DNA (lane 5), control DNA (lane 6); (b) in the presence of ascorbic acid (10 μM) 250 μM **2** + DNA (lane 1), 200 μM **2** + DNA (lane 2), 150 μM **2** + DNA (lane 3), 100 μM **2** + DNA (lane 4) and 50 μM **2** + DNA (lane 5), control DNA (lane 6).

complexes. Due to the resemblance between the electrochemical and biological reactions, CV provides a useful complement to study the binding of metal complexes to DNA, in addition to other spectroscopic methods of investigation. The cyclic voltammograms (Figs. 8 and 9) of complexes **1** and **2** show cathodic and anodic peaks due to the reduction of M^{II} and its subsequent oxidation. In the absence of CT-DNA, complex **1** exhibits a quasireversible redox wave for a one-electron transfer process corresponding to the Co^{II}/Co^{I} redox couple with an anodic peak potential E_{pa} of −0.27 V and a cathodic peak potential of −0.35 V. The formal potential $E_{1/2}$ taken as an average of anodic and cathodic peak values is −0.310 V and the corresponding ΔE_p value was 0.08 V. No appreciable change was observed at different scan rates. In the presence of CT-DNA, there is a shift in ΔE_p value (0.16 V) as well as in the $E_{1/2}$ value (−0.28 V), indicative of strong binding of the complex to CT-DNA. The cyclic voltammogram of complex **2** also reveals a one-electron quasireversible behaviour with $E_{1/2} = -0.33$ V and $\Delta E_p = 0.16$ V ($E_{pa} = -0.25$ V and $E_{pc} = -0.41$ V) [47]. In the presence of

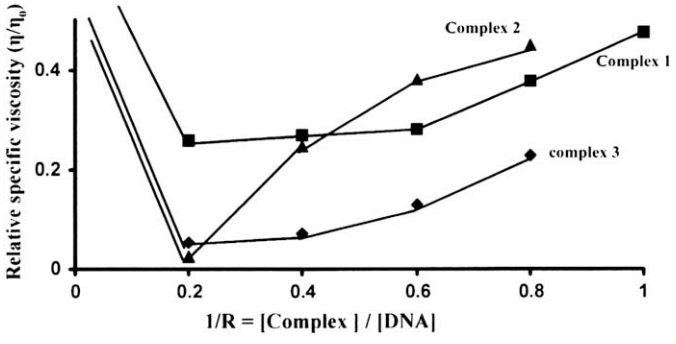

Fig. 7. Effects of increasing amount of complex **1** (■), complex **2** (▲) and complex **3** (◆) on the relative viscosity of CT-DNA at 29 ± 0.1 °C. [DNA] = 0.25 × 10^{-4} M, [M] = 0.05–0.25 × 10^{-4} M.

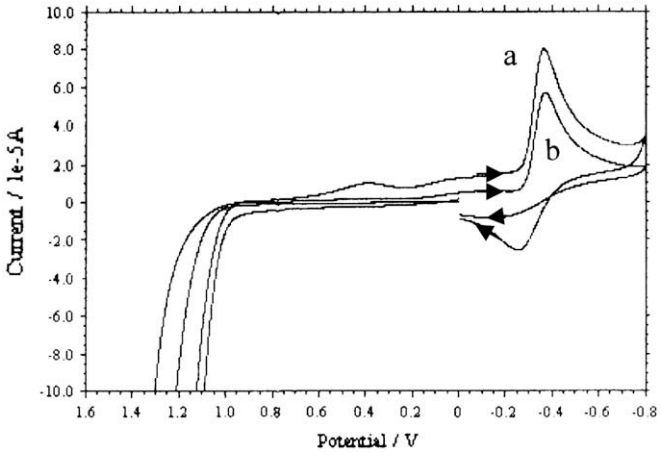

Fig. 8. Cyclic voltammograms at a scan rate 0.2 V s^{-1} in DMSO/H_2O (5:95) (a) free complex **1**, (b) complex **1** in the presence of CT-DNA.

DNA, reversibility of the electron transfer was maintained with a significant shift in ΔE_p value (0.15 V) as well as in $E_{1/2}$ value (−0.375 V). In addition to the changes in the formal potential, the peak currents in the cyclic voltammograms of both the complexes decreased than those in the absence of DNA, indicating a strong binding of complexes **1** and **2** with DNA.

From reversible redox reactions of the free and bound species, the corresponding equilibrium constants for binding of each oxidation state to DNA can be obtained from the Nernst equation.

$$E_b^o - E_f^o = 0.059 \log(K_{1+}/K_{2+})$$

Where E_b^o and E_f^o are the formal potentials of M^{II}/M^{I} couple, in the free and bound forms, respectively, and K_{1+} and K_{2+} are the corresponding binding constants for +1 and +2 species to DNA. K_{1+}/K_{2+} has been determined using the above equation and found to be 3.22 and 5.76 for complexes **1** and **2**, respectively, whose potential shifts are 0.03 V and 0.045 V, respectively.

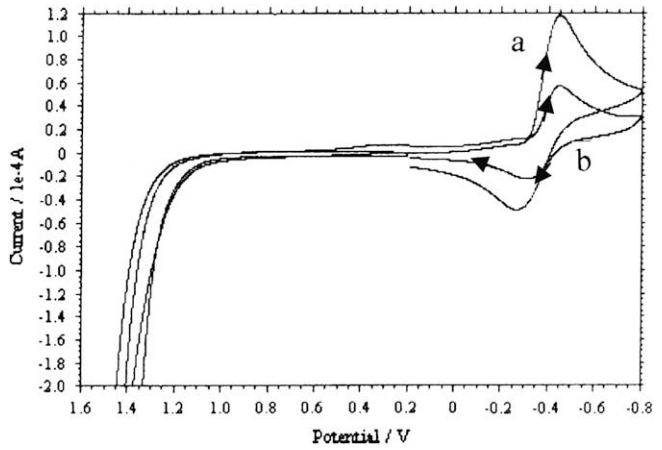

Fig. 9. Cyclic voltammograms at a scan rate 0.2 V s^{-1} in DMSO/H_2O (5:95) (a) free complex **2**, (b) complex **2** in the presence of CT-DNA.

3. Experimental

3.1. Chemistry

3.1.1. Materials

Reagent grade chemicals were used without further purification for all syntheses. $CoCl_2 \cdot 6H_2O$, $CuCl_2 \cdot 2H_2O$, $ZnCl_2$, K_2CO_3, KI, 1,2-dibromoethane, diethyloxalate, tris-base (Merck), 2-mercaptobenzimidazole (Sigma–Aldrich Chemie) were used as received and Calf thymus DNA (CT-DNA) was obtained from Sigma.

3.1.2. Physical measurements

Microanalysis (%CHN) was performed on a carlo Erba analyzer model 1108. Molar conductances were measured at room temperature with a Digisun electronic conductivity bridge. Infra red spectra were collected by using KBr pellets on an Interspec 2020 FT-IR spectrometer. USB 2000-Ocean optics spectrometer was used to record the electronic spectra. ^1H and ^{13}C spectra were recorded on a Bruker DRX-300 spectrometer at 300 MHz. Chemical shifts were reported on the δ scale in parts per million (ppm). The EPR spectrum of the copper complex was acquired on a Varian E 112 spectrometer using X-band frequency (9.1 GHz) at liquid nitrogen temperature in solid state. The electrospray mass spectra were recorded on a Micromass Quattro II triple quadrupol mass spectrometer. Emission spectra were determined with a Hitachi F-2500 fluorescence spectrophotometer. Cyclic voltammetry was performed on CH-instrument electrochemical analyzer. The supporting electrolyte was 0.4 M KNO_3 in water. All samples were purged with nitrogen prior to measurements at room temperature. A three-electrode configuration that comprised of a Pt micro cylinder as a working electrode, Pt wire as auxiliary electrode and an Ag/AgCl electrode as a reference electrode was used.

3.1.3. DNA binding experimental

All the experiments involving the interaction of the complexes with DNA were conducted in aerated Tris–HCl buffer (0.01 M, pH 7.2). Solutions of calf thymus DNA in buffer gave a ratio of UV absorbance at 260 and 280 nm of ca. 1.9:1 indicating that DNA was free from protein [48]. DNA concentration per nucleotide was determined by the extinction coefficient 6600 $dm^3\,mol^{-1}\,cm^{-1}$ at 260 nm. Absorption spectral titration experiments were performed by maintaining a constant concentration of the complex and varying the nucleic acid concentration. This was achieved by diluting an appropriate amount of the metal complex solutions and DNA stock solutions while maintaining the total volume constant. This results in a series of solutions with varying concentrations of DNA but a constant concentration of the complex. The absorbance (A) was recorded after successive additions of CT-DNA on Shimadzu UV-1700 pharmaspec UV–vis spectrophotometer using cuvettes of 1 cm path length. While measuring the absorption spectra an equal amount of DNA was added to both the compound solution and the reference solution to eliminate the absorbance of the DNA itself. The intrinsic binding constant K_b of the complex to CT-DNA was determined from Eq. (7) [49] through a plot of [DNA]/($\varepsilon_a - \varepsilon_f$) vs. [DNA]

$$\frac{[\mathrm{DNA}]}{\varepsilon_a - \varepsilon_f} = \frac{[\mathrm{DNA}]}{\varepsilon_b - \varepsilon_f} = \frac{1}{K_b\left(\varepsilon_b - \varepsilon_f\right)} \tag{7}$$

where [DNA] is the concentration of DNA in base pairs, ε_a, ε_f and ε_b are, respectively, the apparent extinction coefficient (A_{obs}/[M]), the extinction coefficient of the free metal (M) complex and the extinction coefficient for the metal (M) complex in the fully bound form. In plots of [DNA]/($\varepsilon_a - \varepsilon_f$) vs. [DNA], K_b is given by the ratio of the slope to the intercept.

Fluorescence spectral measurements were carried out using Hitachi F-2500 spectrofluorimeter. The Tris buffer was used as a blank to make preliminary adjustments. The excitation wavelength was fixed and the emission range was adjusted before measurements. To compare quantitatively the binding affinity of the complexes to DNA, the intrinsic binding constant K_b were obtained by titrating fixed amounts of complexes in the presence of EB with increasing amounts of DNA. An excitation wavelength of 510 nm was used, and the total fluorescence emission was monitored at 590 nm. The observed binding constant K_{obs} of EB was computed from the scatchard plots and from the replot of K_{obs} intrinsic binding constant K_b of the complexes was estimated. Further support for the complex binding to DNA was obtained from emission quenching experiments.

The cleavage of supercoiled pBR322 DNA in the absence of activating agents was observed using gel electrophoresis. In reactions using supercoiled pBR322 DNA (300 ng) in Tris–HCl (10 mmol) buffer at pH 7.4 was treated with complex **2** (50–250 μM). The samples were incubated for 1 h at 37 °C. A loading buffer containing 25% bromophenol blue, 0.25% xylene cyanol, 30% glycerol was added and electrophoresis was carried out at 100 V for 2 h in Tris–HCl buffer using 1% agarose gel containing 1.0 μg/ml ethidium bromide.

The DNA cleavage with added reductant ascorbic acid was monitored as in case of cleavage experiment without added reductant using agarose gel electrophoresis. Reactions using pBR322 DNA in Tris–HCl buffer at pH 7.4 were treated with complex **2** (50–250 μmol) and ascorbic acid (10 μmol). The samples were incubated for 1 h at 37 °C.

All the gels were viewed by UVP gel doc system and photographed.

Viscosity measurements were carried out using an Ostwald's capillary viscometer at 29 ± 0.01 °C. Several time readings were obtained at each titration point and an average flow time was calculated. Data were presented as (η/η_0) vs. the binding ratio ([M]/[DNA]), [50] were η is the viscosity of DNA in the presence of the complex and η_0 is the viscosity of DNA alone. Viscosity values were calculated from the observed flow time of DNA containing solution ($t > 100$ s), corrected for the flow time of the buffer alone (t_0), $\eta = t - t_0$.

3.1.4. Syntheses

3.1.4.1. N,N-Bis(2-mercaptobenzimidazolyl) oxalate hydrochloride (L_1). Ligand L_1 was synthesized according to the

reported procedure [16] as described below (Scheme 1). To a methanolic solution of 2-mercaptobenzimidazole (5.00 g, 33 mmol), diethyloxalate (2.26 cm^3, 16 mmol) was added in a 2:1 molar ratio. The solution was heated under reflux for ca. 1 h. After cooling, conc. HCl (6 cm^3) was added dropwise with stirring. The cream crystalline product formed, was filtered off, washed thoroughly with hexane and dried *in vacuo*. L_l, yield: 76.2%; m.p. 100 °C. Anal. calc. for $C_{16}H_{10}N_4O_2S_2\cdot 3HCl\cdot CH_3OH$ (494.65): C, 41.27; H, 3.46; N, 11.36. Found: C, 41.13; H, 3.43; N, 11.32. IR (KBr, cm^{-1}): ν_{max} 2368 (S–H), 1523 (C=N), 1353 (C–N), 1625 (C=O), 739 (C–S). UV–vis [DMSO; λ_{max}/nm] 247, 273. ^{1}H NMR (300 MHz, DMSO, 25 °C): δ_H: 2.95 (SH); 7.38–7.69 (Ar–H). ^{13}C NMR (75.47 MHz, DMSO-d_6): δ 160.96 (C=O); 112.96, 125.03, 132.47 (Ar–C). ESI-MS (*m/z*) 494 ($C_{16}H_{10}N_4O_2S_2\cdot 3HCl\cdot CH_3OH + H^+$), 429 ($C_{16}H_{10}N_4O_2S_2\cdot 2H Cl + 2H^+$).

3.1.4.2. 2,2,2′,2′-S,S[Bis(bis-N,N-2-thiobenzimidazolyl oxalato-1,2-ethane)] (L_2). A mixture of L_1, (4.62 g, 10 mmol) 1,2-dibromoethane (0.86 cm^3, 10 mmol), anhydrous K_2CO_3 (1.38 g, 10 mmol) and KI in acetonitrile was stirred for ca. 24 h at 35 ± 5 °C. The reaction mixture was poured into water, made alkaline with NaOH solution. The TLC pure compound was isolated, washed with H_2O and dried *in vacuo*. L_2, yield: 53.2%; m.p. 190 °C. Anal. calc. for $C_{36}H_{24}N_8O_4S_4\cdot CH_3 CN\cdot H_2O$ (819.93): C, 55.66; H, 3.56; N, 15.37. Found: C, 55.53; H, 3.51; N, 15.64. IR (KBr, cm^{-1}): ν_{max}: 2853 (CH_2), 1517 (C=N), 1362 (C–N), 1619 (C=O), 737 (C–S). UV–vis [DMSO; λ_{max}/nm] 245, 270. ^{1}H NMR (300 MHz, DMSO-d_6, 25 °C): δ_H: 2.75 (S–CH_2–CH_2–S); 7.15–7.51 (Ar–H). ^{13}C NMR (75.47 MHz, DMSO-d_6): δ: 151.24 (C=O); 113.66, 121.29, 139.25 (Ar–C); 39.50 (CH_2). ESI-MS (*m/z*) 817 ($C_{36}H_{24}N_8O_4S_4\cdot CH_3CN\cdot H_2O - 2H^+$), 775 ($C_{36}H_{24}N_8O_4 S_4\cdot H_2O\cdot - 3H^+$).

*3.1.4.3. 2,2,2′,2′-S,S[Bis(bis-N,N-2-thiobenzimidazolyloxalato-1,2-ethane)cobalt(II)]chloride (**1**).* Ligand L_2 (1.9 g, 25 mmol) and $CoCl_2$ (1.36 g, 50 mmol) were dissolved in 20 cm^3 MeOH. The solution was heated to reflux for 24 h, resulting in a clear blue solution. Slow evaporation of the solution afforded a deep blue TLC pure crystalline compound. Yield: 55%; m.p. 240 °C. Anal. calc. for $C_{36}H_{24}N_8O_4S_4Cl_4Co_2$ (1020.55): C, 42.36; H, 2.37; N, 10.97. Found: C, 42.79; H, 2.43; N, 12.61. IR (KBr, cm^{-1}): ν_{max}: 2923 (CH_2), 1496 (C=N), 1593 (C=O), 704 (C–S), 509 (Co–O). UV–vis [DMSO; λ_{max}/nm, 10^{-3} M] 242, 290, 680 ($\varepsilon = 448\ M^{-1}\ cm^{-1}$). Mmo_M (DMSO) 130.5 $\Omega^{-1}\ cm^2\ mol^{-1}$ (1:4 electrolyte). ESI-MS (*m/z*) 1019 $[M - H^+]$, 981 $[M - Cl^-]^{1+}$, 478 $[M - 2Cl^-]^{2+}$, 224, 222 $[M - 4Cl^-]^{4+}$.

*3.1.4.4. Dichloro-2,2,2′,2′-S,S[bis(bis-N,N-2-thiobenzimidazolyloxalato-1,2-ethane)copper(II)] (**2**).* As described for **1** using $CuCl_2$ (0.85 g, 50 mmol) afforded a green compound. Yield: 62%. m.p. 210 °C. Anal. calc. for $C_{36}H_{24}N_8O_4S_4Cl_4Cu_2$. (1029.77): C, 41.98; H, 2.34; N, 10.88. Found: C, 42.17; H, 2.35; N, 11.21. IR (KBr, cm^{-1}): ν_{max}: 2918 (CH_2), 1493 (C=N), 1587 (C=O), 710 (C–S), 504 (Cu–O). UV–vis [DMSO; λ_{max}/nm,10^{-3} M] 243, 276, 800 ($\varepsilon = 83\ M^{-1}\ cm^{-1}$). Mmo_M (DMSO) 26.5 $\Omega^{-1}\ cm^2\ mol^{-1}$ (non-electrolyte).

*3.1.4.5. Dichloro-2,2,2′,2′-S,S[bis(bis-N,N-2-thiobenzimidazolyloxalato-1,2-ethane)zinc(II)] (**3**).* As described for **1** using anhydrous $ZnCl_2$ (0.68 g, 50 mmol) gave cream coloured compound. Yield: 70.0%; m.p. 280 °C. Anal. calc. for $C_{36}H_{24}N_8O_4S_4Cl_4Zn_2$ (1033.47): C, 41.83; H, 2.34; N, 10.84. Found: C, 42.68; H, 2.17; N, 11.42. IR (KBr, cm^{-1}): ν_{max}: 2918 (CH_2), 1491 (C=N), 1587 (C=O), 718 (C–S), 493 (Zn–O). UV–vis [DMSO; λ_{max}/nm, 10^{-3} M] 244, 289. ^{1}H NMR (300 MHz, DMSO-d_6, 25 °C): δ_H: 2.80 (S–CH_2–CH_2–S); 7.19–7.27 (Ar–H). ^{13}C NMR (75.47 MHz, DMSO-d_6): δ 164.27 (C=O); 115.91, 122.27, 135.47 (Ar–C); 37.53 (CH_2). Mmo_M (DMSO) 23.7 $\Omega^{-1}\ cm^2\ mol^{-1}$ (non-electrolyte).

4. Conclusion

The interactions of complexes **1–3** with CT-DNA were examined by various techniques, and the results suggest that the complexes bind to DNA mainly through partial intercalation binding mode. Besides this, complex **2** shows efficient ''artificial nuclease activity''. We propose that the macrocyclic complexes bearing biologically significant benzimidazole group are promising therapeutic drug candidates. These studies form an important rationale for drug design and warrant further in vivo experiments and pharmacological assays.

Acknowledgements

We are grateful to the Council of Scientific and Industrial Research, New Delhi (research grant No. 01/(1982)/05-EMR-II) for the financial support. We are highly indebted to the Regional Sophisticated Instrumentation Center, Central Drug Research Institute, Lucknow for providing CHN analysis data, ESI-Mass and NMR spectra, and Regional Sophisticated Instrumentation Center, Indian Institute of Technology, Bombay for EPR measurements. The authors gratefully acknowledge Prof. Javeed Mussarat, Department of Microbiology and Syed Faiz Zaidi, Aligarh Muslim University, Aligarh, India for providing Gel Electrophoresis facility and improving the English language of the manuscript, respectively.

References

[1] (a) L. Ronconi, P.J. Sadler, Coord. Chem. Rev. 251 (2007) 1633;
(b) T. Storr, K.H. Thompson, C. Orvig, Chem. Soc. Rev. 35 (2006) 534;
(c) Z.J. Guo, P.J. Sadler, Angew. Chem. Int. Ed. 38 (1999) 1513.
[2] M.A. Koch, A. Schuffenhauer, M. Scheck, S. Wetzd, M. Casaulta, A. Odermatt, P. Ertl, H. Waldmann, Proc. Natl. Acad. Sci. U.S.A. 102 (2005) 17272.
[3] G.I. Miessler, D.A. Tarr, Inorganic Chemistry, third ed. Prentice Hall, 2003, pp. 299–336.
[4] E. Meggers, Curr. Opin. Chem. Biol. 11 (2007) 287.
[5] (a) A.A. Spasov, I.N. Iyzhista, L.I. Bugaeva, V.A. Anisimova, Khim-Farm. Zh. 33 (1999) 6;

(b) F. Gumus, O. Algul, G. Eren, H. Eroglu, N. Diril, S. Gur, A. Ozkul, Eur. J. Med. Chem. 38 (2003) 473.
[6] (a) S. Demirayak, U.A. Mohsen, A.C. Karaburum, Eur. J. Med. Chem. 37 (2002) 255;
(b) L. Garuti, M. Roberti, M. Malagoli, T. Rossi, M. Castelli, Bioorg. Med. Chem. Lett. 14 (2004) 1253;
(c) S.M. Sondhi, N. Singh, A. Kumar, O. Lozach, L. Meijer, Bioorg. Med. Chem. 14 (2006) 3758;
(d) C. Beaulieu, Z. Wang, D. Denis, G. Greig, S. Lamontagne, G. O'Neill, D. Slipetz, J. Wang, Bioorg. Med. Chem. Lett. 14 (2004) 3195.
[7] A. Hori, Y. Imaeda, K. Kubo, M. Kusaka, Cancer Lett. 183 (2002) 53.
[8] K. Vernagy, I. Sovago, K. Agoston, Z. Liko, H. Suli-Vargha, D. Sanna, G. Micera, J. Chem. Soc., Dalton Trans. (1994) 2939.
[9] E. Amtmann, M. Zoller, H. Wesch, G. Schilling, Cancer Chemother. Pharmacol. 47 (2001) 461.
[10] M.F. Brana, M. Cacho, A. Gradillas, B. de Pascual-Teresa, A. Ramos, Curr. Pharm. Des. 7 (2001) 1745.
[11] B. Lippert (Ed.), Cisplatin, Chemistry and Biochemistry of a Leading Anticancer Drug, Wiley-VCH, Weinheim, 1999 and references therein.
[12] J. Liu, X.H. Zou, Q.L. Zhang, W.J. Mei, J.Z. Liu, L.N. Ji, Met Based Drugs 7 (2000) 343.
[13] U. Pindur, M. Haber, K. Sattler, J. Chem. Educ. 70 (1993) 263.
[14] A. Sparsky, D.S. Sigman, Biochemistry 24 (1985) 8050.
[15] C.J. Burrows, J.G. Muller, Chem. Rev. 98 (1998) 1109.
[16] F. Arjmand, B. Mohani, S. Ahmad, Eur. J. Med. Chem. 40 (2005) 1103.
[17] S.M. Sondhi, M. Johar, R. Shukla, R. Raghubir, N. Bharti, A. Azam, Aust. J. Chem. 54 (2001) 461.
[18] S.M. Annigeri, A.D. Naik, U.B. Gangadharmath, V.K. Revankar, V.B. Mahale, Transition Met. Chem. 27 (2002) 316.
[19] X. Ottenwaelder, A. Aukauloo, Y. Journaux, R. Carrasco, J. Cano, B. Cervera, I. Castro, S. Curreli, M.C. Munoz, A.L. Rosello, B. Soto, R.R. Garcia, Dalton Trans. (2005) 2516.
[20] R.M. Silverstein, G.C. Bassler, T.C. Morill, Spectrometric Identification of Organic Compounds. 3rd ed. John Wiley and Sons, Inc., 1974, p. 179.
[21] M. Vaidyanathan, R. Balamurugan, U. Sivagnanam, M. Palanaindavar, J. Chem. Soc., Dalton Trans. (2001) 3498.
[22] G. Rajsekhar, C.P. Rao, P. Saarenketo, K. Nattinen, K. Rissanen, New J. Chem. 28 (2004) 75.
[23] S. Chandra, Sangeetika, S. Thakur, Transition Met. Chem. 29 (2004) 925.
[24] B.J. Hathaway, D.E. Billing, Coord. Chem. Rev 5 (1970) 143.
[25] A. Romerosa, C. S-Bello, M.S. -Ruiz, A. Caneschi, V. Mckee, M. Peruzzini, L. Sorace, F. Zanibini, Dalton Trans. (2003) 3233.
[26] A.B.P. Lever, Inorganic Electronic Spectroscopy, Elsevier Publishing Company, Amsterdam, London NY, 1968, p. 61.
[27] J.K. Barton, A.T. Danishefsky, J.M. Goldberg, J. Am. Chem. Soc. 106 (1984) 2172.
[28] C.S. Chow, J.K. Barton, Methods Enzymol. 212 (1992) 219.
[29] B.D. Wang, Z.Y. Yang, T.R. Li, Bioorg. Med. Chem. 14 (2006) 6012.
[30] B.D. Wang, Z.Y. Yang, P. Crewdson, D.Q. Wang, J. Inorg. Biochem. 101 (2007) 1492.
[31] J.H. Tan, Y. Lu, Z.S. Huang, L.Q. Gu, J.Y. Wu, Eur. J. Inorg. Chem. 42 (2007) 1169.
[32] (a) M. Baldini, M.B. Ferrari, F. Bisceglie, G. Pelosi, S. Pinelli, P. Tarasconi, Inorg. Chem. 42 (2003) 2049;
(b) A.K. Patra, S. Dhar, M. Nethaji, A.R. Chakrvarty, Dalton Trans. (2005) 896.
[33] V. Rajendiran, M. Surali, E. Suresh, S. Sinha, K. Somasundaram, M. Palanaindavar, Dalton Trans. (2008) 148.
[34] J.B. Le Pecq, C. Paoletti, J. Mol. Biol. 27 (1967) 87.
[35] Y. Wang, Z.N. Yang, Z.N. Chen, Bioorg. Med. Chem. Lett. 18 (2008) 298.
[36] Z.Y. Yang, B.D. Wang, Y.H. Li, J. Organomet. Chem. 691 (2006) 4156.
[37] J.R. Lakowiez, G. Webber, Biochemistry 12 (1973) 4161.
[38] H. Li, X.Y. Le, D.W. Pang, H. Deng, Z.H. Xu, Z.H. Lin, J. Inorg. Biochem. 99 (2005) 2240.
[39] K.J. Humphreys, A.E. Johnson, K.D. Karlin, S.E. Rokita, J. Biol. Inorg. Chem. 7 (2002) 835.
[40] L.M. Mirica, X. Ottenwealder, T.D.P. Stack, Chem. Rev. 104 (2004) 1013.
[41] S. Satyanarayana, J.C. Dabrowiak, J.B. Chaires, Biochemistry 31 (1992) 9319.
[42] S. Satyanarayana, J.C. Dabrowiak, J.B. Chaires, Biochemistry 32 (1993) 2573.
[43] C.R. Brodie, J. Collins, J.R.A. -Wright, Dalton Trans. (2004) 1145.
[44] C.S. Allardyce, P.J. Dyson, D.J. Ellis, S.L. Heath, Chem. Commun. (2001) 1396.
[45] J. Liu, J.B. Lu, H. Li, Q.-L. Zhang, L.-N. Ji, J.-X. Zhang, L.-H. Qu, H. Zhou, Transition Met. Chem. 27 (2002) 687.
[46] J. Liu, H. Zhang, C. Chen, H. Deng, T. Lu, L. Ji, Dalton Trans. (2003) 114.
[47] X. Lu, K. Zhu, M. Zhang, H. Liu, J. Kang, J. Biochem. Biophys. Methods 52 (2002) 189.
[48] J. Marmur, J. Mol. Biol. 3 (1961) 208.
[49] A. Wolfe, G.H. Shimer, T. Meehan, Biochemistry 26 (1987) 6392.
[50] M. Erikkson, M. Leijon, C. Hiort, B. Norden, A. Groslund, Biochemistry 33 (1994) 5031.